Reactivity of cellulose during hydrothermal carbonization of lignocellulosic biomass

Maurizio Volpe[a,b]*, Antonio Messineo[a], Mikko Mäkelä[c,d], Meredith R. Barr[e], Roberto Volpe[e], Chiara Corrado[f], Luca Fiori[b]

[a]*Facoltà di Ingegneria e Architettura, Università degli Studi di Enna"Kore", Cittadella Universitaria, 94100, Enna, Italy*
[b]*Dipartimento di Ingegneria Civile Ambientale e Meccanica, Università degli Studi di Trento, via Mesiano 77, 38123, Trento, Italy*
[c]*Aalto University, School of Chemical Engineering, Department of Bioproducts and Biosystems, PO Box 16300, 00076 Aalto, Finland*
[d]*Swedish University of Agricultural Sciences, Department of Forest Biomaterials and Technology, Skogsmarksgränd, 90183 Umeå, Sweden*
[e]*Queen Mary University of London, Mile End Road, London E1 4NS, UK*
[f]*UNiversity of Palermo, Department of BioMedicine, Neurosciences and Advanced Diagnostics (Bi.N.D), via Divisi 83, 90133 Palermo, Italy.*
**corresponding author: maurizio.volpe@unikore.it*

Abstract

Hydrothermal carbonization of pure cellulose and birchwood samples was carried out at temperatures between 160 and 280 °C, 0.5 h residence time and biomass-to-water ratio of 20 wt% dry basis, to investigate HTC reactivity of cellulose naturally occurring lignocellulosic biomass. Pure cellulose samples remained unaltered at temperatures up to 220 °C, but significantly decomposed at 230 °C producing a thermal recalcitrant aromatic, high energy-dense material, showing lignin-like behavior. Fourier Transform Infrared spectroscopy (FTIR) showed dehydration and aromatization reactions occurring at temperatures equal or higher than 230 °C for pure cellulose samples while similar increase in aromatization for birchwood hydrochars was evident only at temperatures equal or higher than 260 °C. Acid hydrolysis, Thermogravimetric analysis (TGA) and FTIR suggest that a higher thermal resistance of natural occurring cellulose in birchwood (when compared to pure cellulose sample) could be related to a 'protecting shield' offered by interlinked lignin in the plant matrix.

Keywords: hydrothermal carbonization, solid biofuel, cellulose reactivity, birchwood, acid hydrolysis

Highlights:

HTC induces decomposition of pure cellulose at temperature higher than 220 °C

HTC promotes aromatization of cellulose at temperature equal or higher than 230 °C

Cellulose decomposition in biomass is mitigated by lignin component during HTC

1. Introduction

The unrestrainable growth of global energy demand together with the increasing environmental concern of using fossil fuel sources for energy production has prompted government authorities to issue new regulations and renewable energy share targets. EU-wide targets and policy objectives planned for 2030, within the 2030 climate and energy framework, include: at least 40% cuts in greenhouse gas emissions (from 1990 levels), 32% share for renewable energy and 32.5% improvement in energy efficiency [1]. To reach the EU 2030 targets and, in particular, the renewable energy ones, in the last years the scientific community has boosted the study for the development of new technologies for the production of thermal and electrical energy using alternative renewable sources. Between the different renewable energy sources, biomass and, in particular, residual organic materials offer several advantages. Residual biomass is widely available in large amount at low cost, its conversion into an energy dense bio-fuel and/or valuable carbon material represents an opportunity to decrease the amount of waste with beneficial impact for the environment and human health [2]. Waste biomass exploitation could be highly economically profitable for waste management companies and represents a carbon-neutral and programmable energy source [3]. The conversion of

residual biomass into energy or valuable carbon-rich feedstock is affected by its high moisture content, its perishability and low energy density. Anaerobic digestion (AD) of wet residual biomass to produce methane-rich biogas represents one of the possible and eco-sustainable route for increasing the renewable energy production while decreasing green-house gas emissions [4]. However, the need for high initial investment costs and the requirement for strict operating conditions has limited the widespread of AD, while most of the operating plants are nowadays surviving owing mainly to economic incentives [5]. Thermochemical technologies applied to conversion of residual biomass such as torrefaction [6–8], slow and fast pyrolysis [9–11], gasification [12] or a combination of these technologies [13] have been largely investigated in the last decades but their widespread diffusion mainly failed due to the low energy efficiency, especially for high moisture content biomass, and the low versatility due to the need of very specific operating conditions strictly related to the nature, morphology and physical and chemical composition of feedstock. In the more recent years, wet thermochemical conversion of biomass is attracting more and more interest among scientists and technology developers. Wet pyrolysis, also known as hydrothermal carbonization (HTC), is carried out in water at sub-critical conditions, typically between 180 and 280 °C and at autogenous vapor pressure (10-60 bar). Water, at HTC reaction conditions, promotes dehydration and decarboxylation of biomass, converting wet residual organic material into a carbon-rich solid material, named hydrochar [14–16]. Comparative studies between dry thermochemical conversion and HTC of waste biomass showed that the latter could be more energetically favorable, promoting higher degree of carbonization of feedstock at same reaction temperatures [17]. Moreover, hydrochars display significantly better energy and fuel qualities than the corresponding

78 pyrochars obtained at the same temperatures [18,19]. Since the rediscovery of wet
79 thermochemical treatment of biomass as a valuable process for CO_2 sequestration and
80 production of renewable solid biofuels [20–22], HTC has been used to convert many
81 kinds of waste biomass: lignocellulosic material as olive mill industry wastes [23]
82 loblolly pine [24]; agro-waste such as: tomato peel [25], orange waste [26], wheat straw
83 [27], food waste [28], organic fraction of municipal solid waste [29], paper mill industry
84 wastes [30–32],sewage sludge [33,34] and plastic wastes [35]. Despite the different
85 nature of the treated feedstock, most of the HTC works focused on the influence of the
86 operative variables like temperature, residence time and biomass to water ratio on the
87 energy, chemical and morphological properties of the produced hydrochars for their
88 possible applications as solid bio-fuels and valuable carbon materials (e.g. activated
89 carbons). According to our current knowledge, very few works attempted at describing
90 the evolution of biomass chemical structure during HTC [36], some studies reported the
91 reactivity of biomass macro-components during HTC albeit starting from commercially
92 available single components and none of them studied how biomass macro-constituents
93 reacted and/or interacted when intermeshed in lignocellulosic matrix [37–39].
94 Systematically larger char yields were observed from the pyrolysis of chemically
95 isolated lignin, compared to expected yields from the pyrolysis of lignin embedded in
96 plant material thus demonstrating that an entirely different reaction pathway is involved
97 when the constituents are embedded in plant material [40]. Nevertheless, unveiling the
98 evolution of reactivity of biomass macro-components during HTC is of great
99 importance to predict the properties of produced hydrochars. This work represents the
100 first study that uses TGA, FTIR and acid hydrolysis analysis, to prove that naturally
101 occurring lignin component interconnected in the biomass matrix could play a role in

102 increasing cellulose thermal resistance during HTC thus improving energy properties of
103 hydrochars.

104 **2. Materials and Methods**

105 *2.1 Material preparation and hydrothermal carbonization*

106 HTC of pure cellulose (Sigma Aldrich 50 μm) and dried birchwood, milled with a Retsch
107 SM2000 (Retsch GmbH) and sieved to grain size ≤ 1 mm, was carried out in an unstirred
108 50 ml batch reactor at 160, 180, 200, 220, 230, 240, 260 and 280 °C, fixed 0.5 h residence
109 time and biomass-to-water ratio of 20 wt% on a dry basis. About 6.00 ±0.05 g of dry
110 feedstock was loaded into the reactor and 30 g ±0.5 g of deionized water was added to it.
111 The mixture was carefully mixed, the reactor sealed, purged with pure nitrogen and heated
112 up to the set temperature (temperature increment of about 8-10 °C/min) and left for the
113 set residence time. At the end of the reaction time the system was quenched by placing
114 the reactor on a large stainless steel disk kept at -30 °C and by blowing compressed air to
115 the reactor's walls. Once the system had reached a temperature of 30 °C, the reactor's
116 outlet valve was opened and reaction gas collected in a graduated cylinder, previously
117 filled with water, to evaluate the produced gas volume. The gas mass yield was then
118 calculated assuming that gas was composed only of CO_2. Hydrochar was then collected
119 by filtration and the solid residue dried in a conventional ventilated oven for at least 12
120 hours. Dried hydrochars were stored in sealed glass vials for further analysis and
121 characterization.

122 *2.2 Analytical determination and characterization*

123 The raw materials and hydrochars were subjected to acid hydrolysis to determine the
124 composition in macro-constituents. High Heating Value (HHV), elemental and proximate

125 composition in terms of Volatile Matter (VM), Fixed Carbon (FC) and Ash content and
126 attenuated Total Reflectance (ATR)_FTIR spectroscopy were also performed.

127 For acid hydrolysis the samples were first extracted with acetone according to the
128 guidelines of SCAN-CM 49:03. 250 mL acetone was used in a Soxhlet apparatus with 1
129 g of sample for 2 hours to guarantee removal of extractives and oils remaining on char
130 particles. The monosaccharide and lignin contents of the extractive-free samples were
131 then determined based on the National Renewable Energy Laboratory (NREL)
132 procedure for determination of structural components in biomass [41]. Sugar recovery
133 standards were prepared from analytical grade D-(+)-glucose, D-(+)-xylose, D-(+)-
134 galactose, D-(+)-mannose, L-(+)-arabinose and L-(+)-rhamnose. Hydrolysed monomers
135 were quantified after filtration based on respective peak areas using a Dionex ICS-3000
136 ion chromatograph (Dionex Corp.) and corrected to respective polymeric forms on a
137 dried, as-received basis [41]. Lignin contents were determined as the sum of
138 gravimetrically determined acid-insoluble lignin and acid-soluble lignin, which was
139 quantified with a Shimadzu UV-2550 spectrophotometer (Shimadzu Corp.) at 205 nm.
140 All acetone extractions and subsequent sugar and lignin determinations were performed
141 in duplicate with overall recoveries of 87-107% on a mass basis and a replicate root
142 mean squared error of 1.4% within a range of 0-99% glucan in the samples.

143 FTIR was carried out on a series of samples using a Perkin Elmer Spectrum 400 FT-
144 IR/NIR spectrometer (Perkin Elmer Inc., Tres Cantos, Madrid) in mid-IR mode,
145 equipped with a Universal ATR sampling device containing diamond/ZnSe crystal. The
146 spectra were recorded in the range from 650 to 4000 cm^{-1}, with a resolution of 4 cm^{-1},
147 by averaging 16 scans, spectra were baseline corrected and normalized.

148 The spectra were interpreted using a bilinear principal component analysis (PCA) model
149 based on absorbance units. The normalized transmittance IR spectra (Fig. S1) were first
150 converted into absorbance, further corrected for baseline offsets using the signals within
151 3600-4000 cm^{-1} and then mean centered for PCA (Fig. S2). The PCA results were given
152 through sample scores on the orthogonal principal components (PCs) and the respective
153 changes in the IR spectra illustrated through orthonormal PC loadings. The interested
154 reader is referred to the published literature on further details on the PCA method
155 [42,43].

156 Ultimate analyses were performed using a LECO 628 analyser equipped with Sulphur
157 module for CHN (ASTM D-5373 standard method) and S (ASTM D-1552 standard
158 method) content determination.

159 The HHV of solid samples was evaluated according to the CEN/TS 14918 standard by
160 means of an IKA C 200 calorimeter. Hydrochar mass yield (Sy) was calculated
161 according to Eq. (1):

162 $$Sy = M_{HCdb}/M_{Rdb} \quad (1)$$

163 where M_{HCdb} represents the mass (dry basis) of the solid remaining after thermal
164 treatment (*i.e.* hydrochar), and M_{Rdb} represents the mass (dry basis) of the raw sample
165 before thermal treatment. Similarly, gas mass yield (Gy) was defined as the mass of gas
166 produced per unit mass of dry raw biomass sample. Liquid mass yield (Ly) was
167 calculated as the complement to 1 of the sum of Sy and Gy. The energy densification
168 ratio (EDR) was calculated according to Eq. (2), where HHV_{HCdb} represents the higher
169 heating value of hydrochar on a dry basis and HHV_{Rdb} represents the higher heating
170 value of the raw material. Energy yield (EY) was calculated according to Eq. (3).

171 $EDR = HHV_{HCdb}/HHV_{Rdb}$ (2)

172 $Ey = EDR*Sy$ (3)

173 Proximate analysis was carried out by means of TGA using a TA Instruments Q500
174 TGA. Between 2 and 20 mg of sample were placed in a 100 μL platinum sample pan,
175 held at room temperature under high purity nitrogen at 60 mL/min (with an additional
176 40 mL/min balance protective gas) for 15 minutes, and then heated at 15 °C/min to 105
177 °C and held for 20 minutes at this temperature to remove moisture. Samples were
178 further heated at 15 °C/min to 900 °C and held for 7 minutes, and then cooled at 15
179 °C/min to 450 °C; the total mass loss from 105 °C through to this point as a portion of
180 the total sample mass on a dry ash-free basis is taken as VM. Samples were then heated
181 up at 15 °C/min to 750 °C in an equivalent flow of air, and held at this temperature for
182 15 min; the remaining mass as a portion of sample mass on a dry basis is taken as ash
183 content. FC on a dry ash-free basis was then calculated by subtracting Ash and VM
184 from the dry mass.

185 Sixteen different experiments (eight for cellulose and eight for birchwood) were carried
186 out at least in triplicate and average results are reported in tables and figures. cellulose
187 and birchwood hydrochars produced at different HTC temperature were coded CE_T
188 and BW_T respectively being "T" the value of process temperature expressed in
189 degrees Celsius.

190 **3. Results**

191 *3.1 Mass yields and hydrochar energy properties*

192 The summary of the results of cellulose and corresponding hydrochars in terms of mass
193 yields, energy properties (HHV, EY and EDR) and elemental, proximate analysis, H/C

194 and O/C atomic ratios are reported in tables 1 and 2 respectively. The data show on the
195 one hand that cellulose did not appreciably degrade during HTC at temperatures lower
196 than 220 °C, on the other hand, that at 230 °C cellulose underwent significant changes
197 in mass yields and energy properties. When HTC temperature was increased from 220
198 to 230 °C, hydrochar mass yield dropped from 82.4 to 55.4 wt%, HHV increased from
199 17.2 MJ/kg to 21.8 MJ/kg, fixed carbon from 3.7 to 42.0 wt%, carbon content increased
200 from 45.8 to 58.8 wt%. More evident changes in cellulose hydrochar composition
201 occurred when temperature was raised to 240 °C, whereby HHV increased to 26.8
202 MJ/kg, however changes were reduced when further rising HTC temperature to 280 °C
203 (HHV = 27.5 MJ/kg). The high changes in energy content and composition could be
204 related to the breaking of the beta-glucosidic covalent bond that reportedly occurs at
205 around 230 °C [36].

206 Table 1 – Cellulose HTC mass yields (wt%, d.b.), energy yields EY and EDR (%) d.b,
207 HHV (MJ/kg) (Mass yields standard deviations < 1.5, HHV standard deviations < 0.05).

Sample	SY	GY	LY*	HHV_{HC}	EY	EDR
CE_raw	-	-	-	16.90	100.0	100.0
CE_160	98.3	0.1	1.6	17.03	99.0	100.8
CE_180	97.5	0.2	2.3	16.96	97.8	100.4
CE_200	95.5	0.2	4.2	16.95	95.8	100.3
CE_220	82.4	0.5	17.1	17.23	84.0	101.9
CE_230	55.4	2.0	42.6	21.76	71.4	128.8
CE_240	51.2	5.4	43.4	26.76	81.1	158.3
CE_260	50.9	7.8	41.3	27.03	81.4	159.9
CE_280	49.2	9.0	41.9	27.46	79.9	162.5

208 *Calculated by difference (LY=100-SY-GY)

209 As shown in table 2, VM, FC, ash content, carbon and hydrogen composition of
210 cellulose hydrochars remained almost unaltered up to 220 °C. This corroborates the

mass yield and energy properties results. The sharp decrease of VM and corresponding increase of FC and C content at 230 °C confirm that a significant change in cellulose chemical composition occurred at that process temperature. Data also demonstrate that when further increasing HTC temperature, FC and C contents slightly increase while H content remains approximately constant or slowly decreases as commonly reported in HTC literature [25,29].

Table 2 – Cellulose raw and hydrochar proximate and elemental analyses. All values except from H/C and O/C atomic ratios in wt% d.b. (standard deviations for proximate and ultimate analysis < 1.2 and 0.2, respectively).

Sample	VM	FC	ASH	C	H	N	O*	H/C	O/C
CE_raw	97.7	2.4	0.0	45.1	5.5	0.0	49.4	1.44	0.82
CE_160	97.9	2.1	0.0	45.1	5.5	0.0	49.4	1.45	0.82
CE_180	97.8	2.2	0.0	45.2	5.5	0.0	49.3	1.45	0.82
CE_200	97.6	2.4	0.0	45.2	5.5	0.0	49.3	1.45	0.82
CE_220	96.3	3.7	0.0	45.8	5.5	0.0	48.7	1.42	0.80
CE_230	58.0	42.0	0.0	58.8	4.6	0.0	36.6	0.94	0.47
CE_240	58.0	42.0	0.0	70.5	3.9	0.1	25.5	0.67	0.27
CE_260	52.8	47.2	0.0	72.2	3.9	0.1	23.8	0.65	0.25
CE_280	52.6	47.4	0.3%	73.2	4.0	0.1	22.4	0.65	0.23

*Calculated by difference O =100-Ash-C-H-N

HTC birchwood mass yields and energy properties results are shown in table 3 and proximate and elemental analysis are shown in table 4. Unlike pure cellulose hydrochars, birchwood hydrochars do not show sharp changes at any specific temperature. Mass yields, HHV, C and FC contents changed gradually with increasing reaction temperature. Significant body of evidence exists in the literature to demonstrate that, during hydrothermal reaction of lignocellulosic biomass, hemicellulose is more reactive than cellulose while lignin component is quite recalcitrant to degradation [37,44].

229 Table 3 – Birchwood HTC mass yields and energy properties (all values in wt% d.b.,
230 mass yields standard deviations < 0.9, HHV standard deviations < 0.3).

Sample	SY	GY	LY*	HHV_{HC}	EY	EDR
BW_raw	-	-	-	18.98	100.0	100.0
BW_160	92.0	0.3	7.7	18.73	90.8	98.7
BW_180	85.4	0.9	13.7	19.06	85.8	100.4
BW_200	70.9	1.6	27.5	20.18	75.4	106.3
BW_220	66.0	2.3	31.7	21.35	74.3	112.5
BW_230	62.3	3.6	34.2	22.69	74.4	119.5
BW_240	57.7	4.1	38.2	24.40	74.2	128.6
BW_260	53.3	7.4	39.3	27.05	75.9	142.5
BW_280	52.1	8.6	39.2	27.89	76.6	146.9

231 *Calculated by difference (LY=100-SY-GY)

232 Table 4 – Birchwood raw and hydrochar proximate and elemental analyses. All values
233 apart from H/C and O/C atomic ratios in wt% d.b. (standard deviations for proximate
234 and ultimate analysis < 1.6 and 0.2, respectively).

Sample	VM	FC	ASH	C	H	N	O*	H/C	O/C
BW_raw	87.8	12.2	0.3	50.4	5.4	0.1	43.8	1.28	0.65
BW_160	88.5	11.5	0.2	50.8	5.5	0.0	43.5	1.29	0.64
BW_180	86.5	13.5	0.2	51.9	5.5	0.1	42.3	1.25	0.61
BW_200	82.2	17.8	0.2	54.7	5.4	0.1	39.6	1.17	0.54
BW_220	77.4	22.6	0.2	57.7	5.2	0.1	37.0	1.08	0.48
BW_230	72.0	28.0	0.2	60.8	5.1	0.1	33.8	0.99	0.42
BW_240	62.4	37.6	0.2	66.5	4.8	0.2	28.4	0.86	0.32
BW_260	54.4	45.6	0.1	71.7	4.6	0.2	23.4	0.77	0.24
BW_280	50.8	49.2	0.1	73.2	4.6	0.2	21.8	0.75	0.22

235 *Calculated by difference O =100-Ash-C-H-N

236 The initial decrease of HTC solid mass yield, faster than that observed for pure
237 cellulose, can be ascribed to the decomposition of extractives and hemicellulose
238 occurring at low HTC temperature (160-200 °C), figure 1.

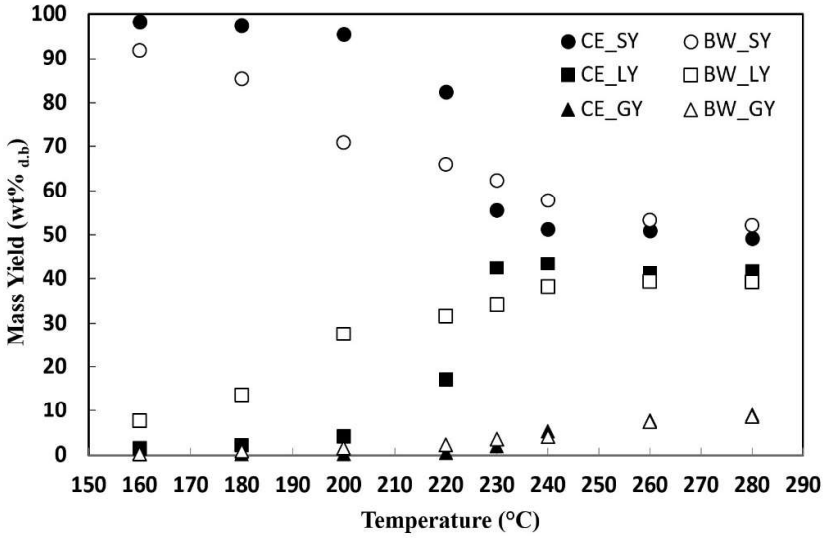

239

240 Fig. 1 Cellulose and birchwood HTC mass yields vs. HTC temperature (SY= solid
241 yield, LY= liquid yield, GY= gas yield)

242 Figure 1 shows the comparison of mass yields changes of pure cellulose and birchwood
243 hydrochars with HTC temperature. Notably, while cellulose solid yield remains
244 approximately constant up to HTC temperature of 220 °C, birchwood hydrochar yield
245 starts decreasing already at 160 °C, due to hydrolysis and/or removal of extractives first
246 and hemicellulose degradation starting at about 180 °C [37]. The decrease of birchwood
247 solid yield results in a liquid yield increase, while gas yields are negligible up to 230 °C
248 and increase slowly up to approximately 9 wt% at 280 °C for both feedstock. After a
249 sharp drop at 230 °C, cellulose hydrochar yields remained constant at approximately 50
250 wt% between 240 and 280 °C, thereby demonstrating that no further significant
251 degradation occurred at temperatures equal to or higher than 240 °C. Conversely,
252 birchwood hydrochar samples showed mass yield progressively decreasing down to 52
253 wt% at a HTC temperature of 280 °C. Mass yields results for both samples are
254 consistent with the production and/or concentration of thermal resistant aromatic
255 material under HTC condition [36,37]. Recent works demonstrated that HTC of residual

biomass occurring at higher temperatures can also improve the rate of back polymerization of organics from the liquid to the solid phase, thus resulting in a decrease of liquid yield and the production of secondary char [45,46].

Figure 2 shows trend in HHV changes vs. HTC temperature for cellulose when compared to birchwood. cellulose hydrochar showed a 56% increase in HHV between 220 and 240 °C, while in the same range of HTC temperature HHV of the corresponding birchwood hydrochars showed an increase of only 14%.

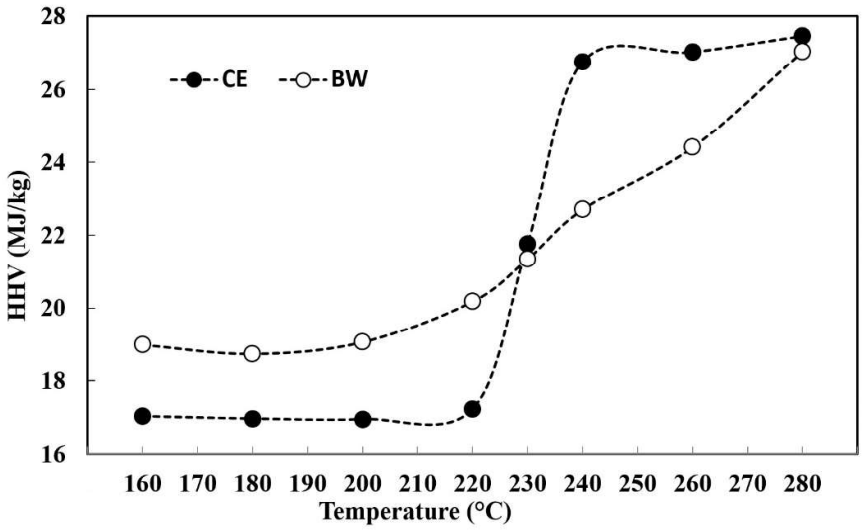

Fig. 2 Cellulose (CE) and birchwood (BW) HHV changes with HTC temperature

Van Krevelen plots for cellulose and birchwood samples reported in figure 3, show the sharp differences in carbonization degree of cellulose hydrochars between the samples produced at temperatures lower than 230 °C and those resulting from HTC performed above 230 °C. Conversely, birchwood hydrochar samples show a progressive carbonization with HTC temperature.

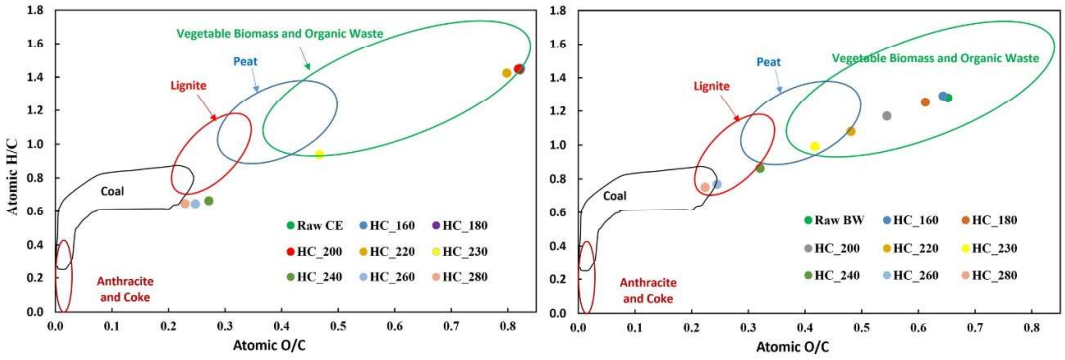

Fig. 3 Van Krevelen plots of Cellulose (left) and Birchwood (right) samples

3.2 Acid hydrolysis

Acid hydrolysis results, reported in table 5, show that the glucose fraction in pure cellulose sample, initially equal to approximately 99 wt%, decreased to 40 wt% at 230 °C and almost disappeared at 240 °C confirming the complete rupture of beta-glycosidic linkage of cellulose. The sharp decrease of the glucose fraction in cellulose hydrochar samples was accompanied by the increase of a lignin-like fraction with the production of more resistant aromatic structured compounds. Acid hydrolysis of birchwood show no evidence of such a sharp drop at 230 °C; conversely, the glucose fraction decreased more gradually with increasing HTC temperature confirming what recently reported in literature [44]. For example, at 240 °C cellulose and birchwood hydrochars showed a glucose fraction of 0.8 and 20.3 wt%, respectively, which suggests a sort of protective effect of the lignin content in the birchwood towards the cellulose content of the same feedstock .

Table 5 – Acid hydrolysis analysis of raw cellulose and birchwood and corresponding hydrochars. All values in wt% d.b. Standard deviation of the data < 2.2.

Sample	Extractives	Lignin	Galactose	Glucose	Xylose	Mannose
CE_raw	0.0	0.0	b.d.l.	98.9	3.0	2.6
CE_160	0.0	0.0	b.d.l.	93.1	2.8	2.5

CE_180	0.0	0.0	b.d.l.	95.7	2.7	2.5
CE_200	0.0	0.0	b.d.l.	96.2	1.8	1.9
CE_220	3.0	9.0	b.d.l.	84.0	0.5	0.9
CE_230	24.0	40.0	b.d.l.	40.2	0.1	0.2
CE_240	21.0	74.0	b.d.l.	0.8	n.a.	n.a.
CE_260	21.0	79.0	b.d.l.	0.1	n.a.	n.a.
CE_280	16.0	79.0	b.d.l.	0.2	n.a.	n.a.
BW_raw	2.0	28.8	1.0	39.4	21.9	1.6
BW_160	4.0	20.5	0.6	43.4	18.3	1.5
BW_180	16.0	17.0	0.3	47.3	7.5	1.0
BW_200	26.0	15.0	0.1	58.7	2.0	0.3
BW_220	26.0	24.0	b.d.l.	52.4	0.2	0.1
BW_230	28.0	31.0	b.d.l.	39.9	0.1	0.1
BW_240	28.0	49.0	b.d.l.	20.3	0.1	0.0
BW_260	34.0	60.0	b.d.l.	1.6	0.1	n.a.
BW_280	34.0	61.0	b.d.l.	0.1	0.0	n.a.

b.d.l.: below detection limits

Figure 4 shows the change of cellulose percentage (normalized by the corresponding hydrochar mass yield) vs. HTC temperature. Cellulose weight percentage in pure cellulose and birchwood hydrochars shows a bi-modal trend depending on the HTC reaction temperature. On the one hand, between 160 and 200 °C, cellulose in both series of hydrochars is approximately constant; on the other hand, between 220 and 260 °C, it decreased quickly, thereby showing linear trends. Notably, cellulose rate of decomposition in birchwood was more than four times slower than pure cellulose hydrochars. The lower rate of cellulose decomposition in birchwood could be associated to the presence of interwoven lignin acting as a protecting shield in the lignocellulosic matrix.

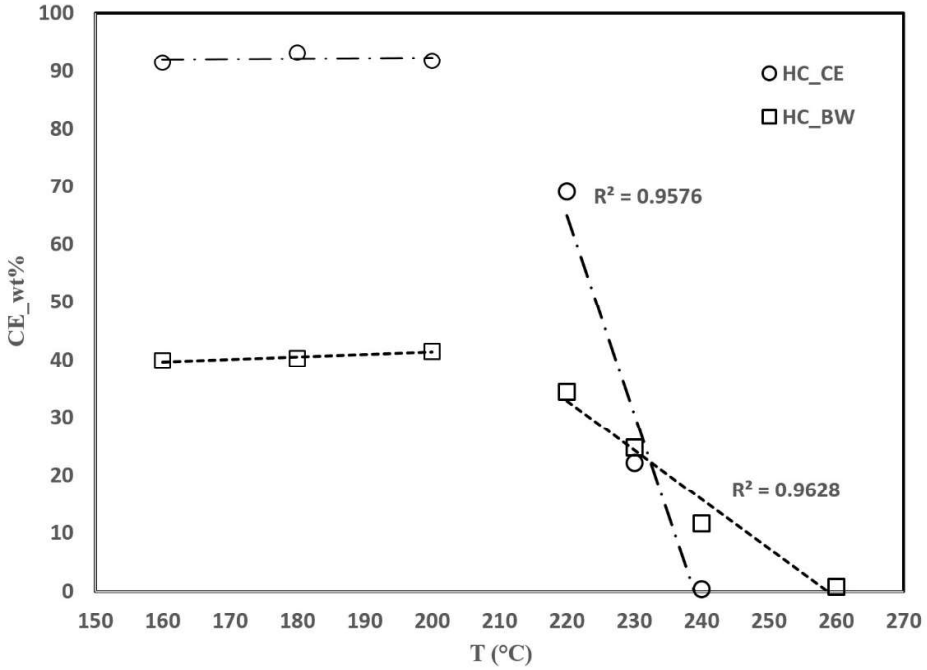

Fig. 4 Normalized cellulose weight component changes with HTC temperature in pure cellulose and birchwood hydrochars

3.3 FTIR analysis

FTIR analysis has been widely used to investigate chemical and structural changes occurring in biomass during HTC [36,47]. The PCA results based on the first two PCs are illustrated in figure 5. In general, positive sample scores in PCA correspond to increased absorbance on positive loadings. The same also applies with negative scores and negative loadings. As illustrated in figure 5, the first PC explained 81% of the variation in the absorbance spectra and mainly separated the samples based on HTC temperature. Higher HTC temperatures hence lead to a decreased adsorbance at around 3300 cm^{-1} attributable to dehydration reactions. Increased absorbance at around 2950-3100 and 790 cm^{-1} can be assigned to sp C-H stretching and bending out of plane modes respectively, testifying a progressive aromatization of hydrochars with HTC temperature. Moreover, the sharp increase of absorbance especially at approximately

1700 and 1215 cm^{-1} can be attributed to the free C=O stretching and bending modes due to cellulose beta-glucosidic linkage breaking [48]. The decrease in absorbance observed at around 1030 cm^{-1} provides evidence that pyranose structure of glucose is lost with increasing HTC temperature [49].

The second PC, which explained approximately 7% of the variation in the spectra, provided mainly a separation between the cellulose and birch wood samples. The cellulose samples showed consistently higher IR absorbance at 1700 and 985 cm^{-1}, probably due to higher concentration of free carbonyl (C=O) and aliphatic (C-O-C ether and alcohol C-O) respectively, due to pyranose structure breaking in cellulose hydrochar samples.

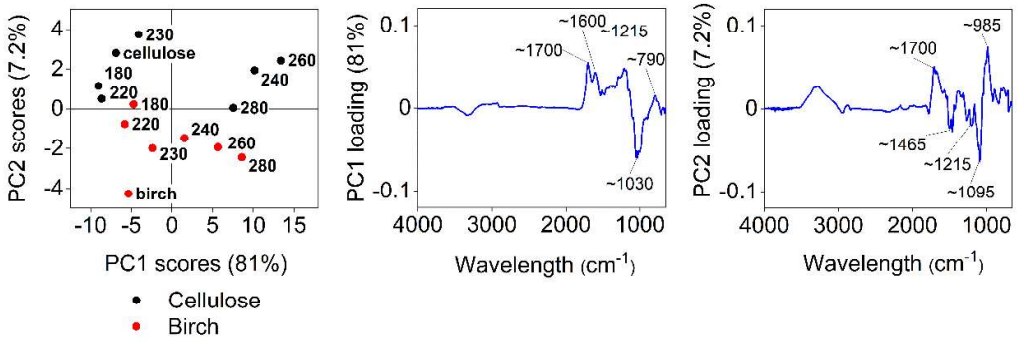

Fig. 5 Sample scores based on the first two PCs and the respective first (middle) and second (right) PC loadings.

3.4 Derivative Thermogravimetric (DTG) analysis and cellulose reactivity

Figure 6a and b show DTG curves of cellulose and birchwood, respectively.

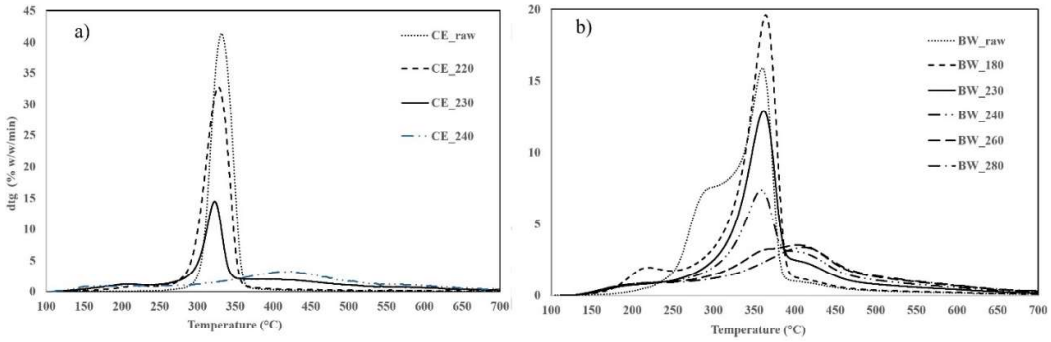

Fig. 6a, b DTG curves of: raw cellulose and selected cellulose hydrochars (a); raw birchwood and selected birchwood hydrochars (b).

Graphs show a sharp decrease in reactivity of cellulose hydrochars above 230 °C and of birchwood hydrochars above 240 °C. It may be noted that all birchwood samples are significantly less reactive than cellulose samples as it is expected owing to the content of lignin in birchwood (cellulose samples obviously do not contain any lignin). In addition, reactivity decreases more sharply and faster with HTC temperature in cellulose hydrochars when compared to birchwood hydrochar. However, the 240 °C birchwood hydrochar sample shows some residual marginally higher reactivity than the pure cellulose hydrochar. Again, probably this is related to the presence of lignin in birchwood and the higher 'resilience' of the compounds formed during carbonisation.

4. Conclusions

This study sheds light on the role of lignin in cellulose decomposition in lignocellulosic biomass. Cellulose component present in naturally occurring biomass matrix is less reactive than free cellulose due to a 'protecting shield' offered by lignin. Mass yields, energy properties, FTIR, DTG and acid hydrolysis analysis demonstrate that pure cellulose is barely affected at a HTC temperature lower than 230 °C (residence time: 0.5 h) but severely degrades at a HTC temperature equal to or higher than 230 °C.

Conversely, natural occurring cellulose in birchwood degrades progressively at increasing HTC temperature, decomposing completely at 280 °C.

Declaration of competing interest

The authors declared that they have no conflicts of interest to this work. We declare that we do not have any commercial or associative interest that represents a conflict of interest in connection with the work submitted.

Acknowledgment

We gratefully acknowledge the help of Paula Seppälä with the acid hydrolyses. This research did not receive any specific grant from funding agencies in the public, commercial, or not-for-profit sectors.

References

[1] European Commision, A policy framework for climate and energy in the period, Communication From the Commission To the European Parliament, the Council, the European Economic and Social Committee and the Committee of the Regions. (2014) 18. http://eur-lex.europa.eu/legal-content/EN/TXT/PDF/?uri=CELEX:52014DC0015&from=EN.

[2] C. Gopu, L. Gao, M. Volpe, L. Fiori, J.L. Goldfarb, Valorizing municipal solid waste: Waste to energy and activated carbons for water treatment via pyrolysis, Journal of Analytical and Applied Pyrolysis. 133 (2018) 48–58. https://doi.org/10.1016/j.jaap.2018.05.002.

[3] N.S. Bentsen, C. Felby, Biomass for energy in the European Union - A review of bioenergy resource assessments, Biotechnology for Biofuels. 5 (2012) 1–10. https://doi.org/10.1186/1754-6834-5-25.

[4] C. Mao, Y. Feng, X. Wang, G. Ren, Review on research achievements of biogas from anaerobic digestion, Renewable and Sustainable Energy Reviews. 45 (2015) 540–555. https://doi.org/10.1016/j.rser.2015.02.032.

[5] L. Yang, F. Xu, X. Ge, Y. Li, Challenges and strategies for solid-state anaerobic digestion of lignocellulosic biomass, Renewable and Sustainable Energy Reviews. 44 (2015) 824–834. https://doi.org/10.1016/j.rser.2015.01.002.

[6] M.J. Prins, K.J. Ptasinski, F.J.J.G. Janssen, Torrefaction of wood Part 2. Analysis of products, Journal of Analytical and Applied Pyrolysis. 77 (2006) 35–40. https://doi.org/10.1016/j.jaap.2006.01.001.

[7] R. Volpe, A. Messineo, M. Millan, M. Volpe, R. Kandiyoti, Assessment of olive wastes as energy source: pyrolysis, torrefaction and the key role of H loss in thermal breakdown, Energy. 82 (2015) 119–127. https://doi.org/10.1016/j.energy.2015.01.011.

[8] V. Benavente, A. Fullana, Torrefaction of olive mill waste, Biomass and Bioenergy. 73 (2015) 186–194. https://doi.org/10.1016/j.biombioe.2014.12.020.

[9] Z. Li, N. Li, W. Yi, P. Fu, Y. Li, X. Bai, Design and operation of a down-tube reactor demonstration plant for biomass fast pyrolysis, Fuel Processing Technology. 161 (2017) 182–192. https://doi.org/10.1016/j.fuproc.2016.12.014.

[10] D. Chiaramonti, M. Prussi, M. Buffi, A.M. Rizzo, L. Pari, Review and experimental study on pyrolysis and hydrothermal liquefaction of microalgae for biofuel production, Applied Energy. 185 (2017) 963–972. https://doi.org/10.1016/j.apenergy.2015.12.001.

[11] R. Volpe, J.M.B. Menendez, T.R. Reina, A. Messineo, M. Millan, Evolution of chars during slow pyrolysis of citrus waste, Fuel Processing Technology. 158 (2017) 255–263. https://doi.org/10.1016/j.fuproc.2017.01.015.

[12] S. You, Y.S. Ok, S.S. Chen, D.C.W. Tsang, E.E. Kwon, J. Lee, C.H. Wang, A critical review on sustainable biochar system through gasification: Energy and environmental applications, Bioresource Technology. 246 (2017) 242–253.

https://doi.org/10.1016/j.biortech.2017.06.177.

[13] M.J. Prins, K.J. Ptasinski, F.J.J.G. Janssen, More efficient biomass gasification via torrefaction, Energy. 31 (2006) 3458–3470. https://doi.org/10.1016/j.energy.2006.03.008.

[14] A. Funke, F. Ziegler, Hydrothermal carbonization of biomass: A summary and discussion of chemical mechanisms for process engineering, Biofuels Bioproduct & Biorefinery. 4 (2010) 160–177. https://doi.org/10.1002/bbb.

[15] A. Kruse, A. Funke, M.-M. Titirici, Hydrothermal conversion of biomass to fuels and energetic materials, Current Opinion in Chemical Biology. 17 (2013) 515–521. https://doi.org/10.1016/j.cbpa.2013.05.004.

[16] S. Román, B. Ledesma, A. Álvarez, C. Coronella, S. V. Qaramaleki, Suitability of hydrothermal carbonization to convert water hyacinth to added-value products, Renewable Energy. 146 (2020) 1649–1658. https://doi.org/10.1016/j.renene.2019.07.157.

[17] M. Volpe, L. Fiori, R. Volpe, A. Messineo, Upgrading of Olive Tree Trimmings Residue as Biofuel by Hydrothermal Carbonization and Torrefaction: a Comparative Study, Chemical Engineering Transaction. 50 (2016) 13–18. https://doi.org/10.3303/CET1650003.

[18] Z. Liu, R. Balasubramanian, Upgrading of waste biomass by hydrothermal carbonization (HTC) and low temperature pyrolysis (LTP): A comparative evaluation, Applied Energy. 114 (2014) 857–864. https://doi.org/10.1016/j.apenergy.2013.06.027.

[19] M. Pecchi, F. Patuzzi, V. Benedetti, R. Di Maggio, M. Baratieri, Thermodynamics of hydrothermal carbonization: Assessment of the heat release profile and process enthalpy change, Fuel Processing Technology. 197 (2020) 106206. https://doi.org/10.1016/j.fuproc.2019.106206.

[20] M.-M. Titirici, A. Thomas, M. Antonietti, Back in the black: hydrothermal carbonization of plant material as an efficient chemical process to treat the CO2 problem?, New Journal of Chemistry. 31 (2007) 787–789. https://doi.org/10.1039/b616045j.

[21] A. Saba, P. Saha, M.T. Reza, Co-Hydrothermal Carbonization of coal-biomass blend: Influence of temperature on solid fuel properties, Fuel Processing Technology. 167 (2017) 711–720. https://doi.org/10.1016/j.fuproc.2017.08.016.

[22] N. Saha, A. Saba, M.T. Reza, Effect of hydrothermal carbonization temperature on pH, dissociation constants, and acidic functional groups on hydrochar from cellulose and wood, Journal of Analytical and Applied Pyrolysis. 137 (2019) 138–145. https://doi.org/10.1016/j.jaap.2018.11.018.

[23] M. Volpe, D. Wüst, F. Merzari, M. Lucian, G. Andreottola, A. Kruse, L. Fiori, One stage olive mill waste streams valorisation via hydrothermal carbonisation, Waste Management. 80 (2018) 224–234. https://doi.org/10.1016/j.wasman.2018.09.021.

[24] M.T. Reza, M.H. Uddin, J.G. Lynam, S.K. Hoekman, C.J. Coronella, Hydrothermal carbonization of loblolly pine: reaction chemistry and water balance, Biomass Conversion and Biorefinery. 4 (2014) 311–321. https://doi.org/10.1007/s13399-014-0115-9.

[25] E. Sabio, A. Álvarez-Murillo, S. Román, B. Ledesma, Conversion of tomato-peel waste into solid fuel by hydrothermal carbonization: Influence of the processing variables, Waste Management. 47 (2016) 122–132. https://doi.org/10.1016/j.wasman.2015.04.016.

[26] E. Erdogan, B. Atila, J. Mumme, M.T. Reza, A. Toptas, M. Elibol, J. Yanik, Characterization of products from hydrothermal carbonization of orange pomace including anaerobic digestibility of process liquor, Bioresource Technology. 196 (2015) 35–42. https://doi.org/doi.org/10.1016/j.biortech.2015.06.115.

[27] M.T. Reza, E. Rottler, L. Herklotz, B. Wirth, Hydrothermal carbonization (HTC) of wheat straw: Influence of feedwater pH prepared by acetic acid and potassium hydroxide, Bioresource Technology. 182 (2015) 336–344. https://doi.org/10.1016/j.biortech.2015.02.024.

[28] T. Wang, Y. Zhai, H. Li, Y. Zhu, S. Li, C. Peng, B. Wang, Z. Wang, Y. Xi, S. Wang, C. Li, Co-hydrothermal carbonization of food waste-woody biomass blend towards biofuel pellets production, Bioresource Technology. 267 (2018) 371–377. https://doi.org/10.1016/j.biortech.2018.07.059.

[29] M. Lucian, M. Volpe, L. Gao, G. Piro, J.L. Goldfarb, L. Fiori, Impact of hydrothermal carbonization conditions on the formation of hydrochars and secondary chars from the organic fraction of municipal solid waste, Fuel. 233 (2018) 257–268. https://doi.org/doi.org/10.1016/j.fuel.2018.06.060.

[30] M. Mäkelä, V. Benavente, A. Fullana, Hydrothermal carbonization of industrial mixed sludge from a pulp and paper mill, Bioresource Technology. 200 (2016) 444–450. https://doi.org/10.1016/j.biortech.2015.10.062.

[31] H. Wikberg, T. Ohra-aho, M. Honkanen, H. Kanerva, A. Harlin, M. Vippola, C. Laine, Hydrothermal carbonization of pulp mill streams, Bioresource Technology. 212 (2016) 236–244. https://doi.org/10.1016/j.biortech.2016.04.061.

[32] Z. Al-Kaabi, R. Pradhan, N. Thevathasan, A. Gordon, Y.W. Chiang, A. Dutta, Bio-carbon production by oxidation and hydrothermal carbonization of paper recycling black liquor, Journal of Cleaner Production. 213 (2019) 332–341. https://doi.org/10.1016/j.jclepro.2018.12.175.

[33] Y. Zhai, X. Liu, Y. Zhu, C. Peng, T. Wang, L. Zhu, C. Li, G. Zeng, Hydrothermal carbonization of sewage sludge: The effect of feed-water pH on fate and risk of heavy metals in hydrochars, Bioresource Technology. 218 (2016) 183–188. https://doi.org/10.1016/j.biortech.2016.06.085.

[34] F. Merzari, M. Langone, G. Andreottola, L. Fiori, Methane production from process water of sewage sludge hydrothermal carbonization. A review. Valorising sludge through hydrothermal carbonization, Critical Reviews in Environmental Science and Technology. 49 (2019) 947–988.

https://doi.org/10.1080/10643389.2018.1561104.

[35] M.E. Iñiguez, J.A. Conesa, A. Fullana, Hydrothermal carbonization (HTC) of marine plastic debris, Fuel. 257 (2019) 116033. https://doi.org/10.1016/j.fuel.2019.116033.

[36] X. Zhuang, H. Zhan, Y. Song, C. He, Y. Huang, X. Yin, Insights into the evolution of chemical structures in lignocellulose and non lignocellulose biowastes during hydrothermal carbonization (HTC), Fuel. 236 (2019) 960–974. https://doi.org/10.1016/j.fuel.2018.09.019.

[37] A.M. Borrero-lópez, E. Masson, A. Celzard, V. Fierro, Modelling the reactions of cellulose, hemicellulose and lignin submitted to hydrothermal treatment, Industrial Crops & Products. 124 (2018) 919–930. https://doi.org/10.1016/j.indcrop.2018.08.045.

[38] X. Lu, P.J. Pellechia, J.R.V. Flora, N.D. Berge, Influence of reaction time and temperature on product formation and characteristics associated with the hydrothermal carbonization of cellulose, Bioresource Technology. 138 (2013) 180–190. https://doi.org/10.1016/j.biortech.2013.03.163.

[39] Y. Gao, X.H. Wang, H.P. Yang, H.P. Chen, Characterization of products from hydrothermal treatments of cellulose, Energy. 42 (2012) 457–465. https://doi.org/10.1016/j.energy.2012.03.023.

[40] A. George, T.J. Morgan, R. Kandiyoti, Pyrolytic Reactions of Lignin within Naturally Occurring Plant Matrices: Challenges in Biomass Pyrolysis Modeling Due to Synergistic Effects, Energy & Fuels. 28 (2014) 6918–6927. https://doi.org/10.1021/ef501459c.

[41] a. Sluiter, B. Hames, R. Ruiz, C. Scarlata, J. Sluiter, D. Templeton, D. Crocker, NREL/TP-510-42618 analytical procedure - Determination of structural carbohydrates and lignin in Biomass, Laboratory Analytical Procedure (LAP). (2012) 17. https://doi.org/NREL/TP-510-42618.

[42] P. Geladi, Chemometrics in spectroscopy. Part 1. Classical chemometrics, Spectrochimica Acta - Part B Atomic Spectroscopy. 58 (2003) 767–782. https://doi.org/10.1016/S0584-8547(03)00037-5.

[43] R. Bro, A.K. Smilde, Principal component analysis, Analytical Methods. 6 (2014) 2812–2831. https://doi.org/10.1039/c3ay41907j.

[44] M. Mäkelä, M. Volpe, R. Volpe, L. Fiori, O. Dahl, Spatially resolved spectral determination of polysaccharides in hydrothermally carbonized biomass, Green Chemistry. 20 (2018) 1114–1120. https://doi.org/10.1039/C7GC03676K.

[45] M. Lucian, M. Volpe, L. Fiori, Hydrothermal Carbonization Kinetics of Lignocellulosic Agro-Wastes: Experimental Data and Modeling, Energies. 516 (2019). https://doi.org/10.3390/en12030516.

[46] M. Volpe, L. Fiori, From olive waste to solid biofuel through hydrothermal carbonisation: The role of temperature and solid load on secondary char formation and hydrochar energy properties, Journal of Analytical and Applied

Pyrolysis. 124 (2017) 63–72. https://doi.org/doi.org/10.1016/j.jaap.2017.02.022.

[47] M.T. Reza, W. Becker, K. Sachsenheimer, J. Mumme, Hydrothermal carbonization (HTC): Near infrared spectroscopy and partial least-squares regression for determination of selective components in HTC solid and liquid products derived from maize silage, Bioresource Technology. 161 (2014) 91–101. https://doi.org/doi.org/10.1016/j.biortech.2014.03.008.

[48] W. Peng, L. Wang, M. Ohkoshi, M. Zhang, Separation of hemicelluloses from Eucalyptus species: Investigating the residue after alkaline treatment, Cellulose Chemistry and Technology. 49 (2015) 757–764.

[49] A. Álvarez-Murillo, E. Sabio, B. Ledesma, S. Rom, Generation of biofuel from hydrothermal carbonization of cellulose. Kinetics modelling, Energy. 94 (2016) 600–608. https://doi.org/10.1016/j.energy.2015.11.024.

Declaration of interests

 The authors declare that they have no known competing financial interests or personal relationships that could have appeared to influence the work reported in this paper.

☐The authors declare the following financial interests/personal relationships which may be considered as potential competing interests:

Supplementary Materials

Reactivity of cellulose during hydrothermal carbonization of lignocellulosic biomass

Maurizio Volpe[a,b]*, Antonio Messineo[a], Mikko Mäkelä[c,d], Meredith R. Barr[e], Chiara Corrado[f], Roberto Volpe[e], Luca Fiori[b]

Fig. S1a, b report FTIR spectra of Cellulose (a) and Birchwood (b) of raw and hydrochars samples at different HTC temperatures.

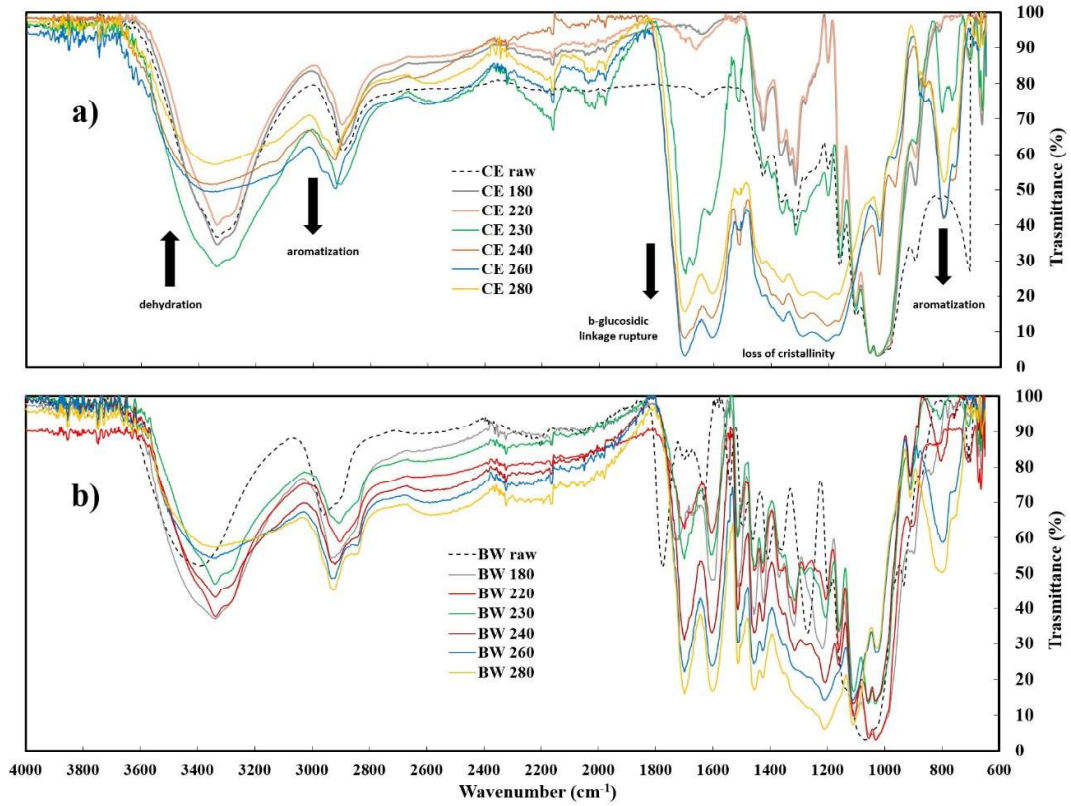

Fig. S1a, b FTIR spectra of Cellulose (a) and Birchwood (b) raw and corresponding hydrochars

Figure S2 reports the normalized FTIR spectra transmittance and their conversion into absorbance spectra for Principal Component Analysis, (PCA) of Cellulose and Birchwood raw and hydrochar samples at different HTC temperature.

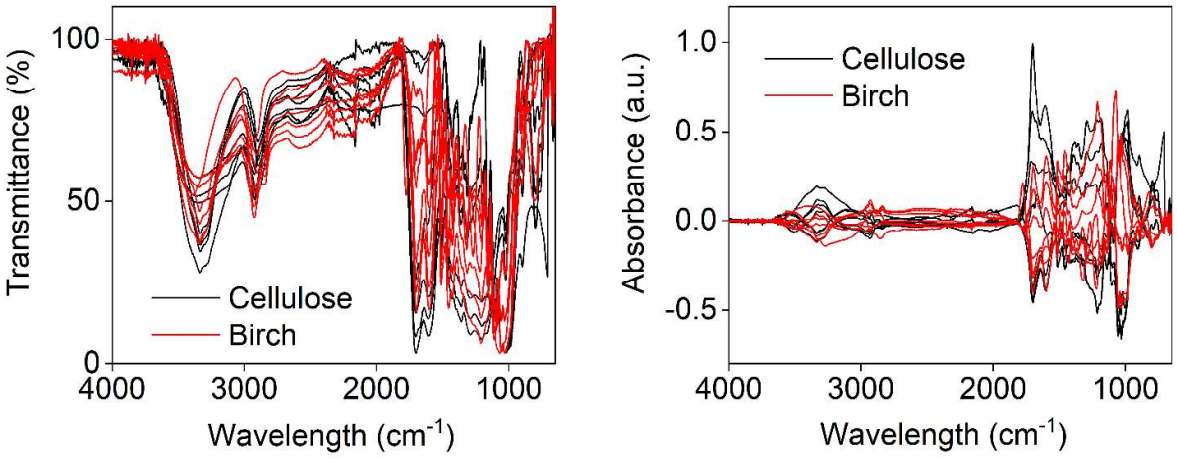

Fig. S2: The FTIR spectra after baseline correction and normalization in transmittance (%, left) and the preprocessed spectra in absorbance units before PCA (right).